Viscoelastic Behaviors and Microstructure of *Sapindus mukorossi* Pericarp for Different Moisture Contents

Mengjiao Xu,[a,b] Cheng Tian,[a] and Daochun Xu [a,b,*]

The viscoelastic behavior of *Sapindus mukorossi* pericarp (the covering of the Indian soapberry fruit) was investigated. Samples were subjected to creep-recovery and oscillatory shear tests. The moisture content had a strong effect on the dynamic moduli, whereas the temperature had little effect. Both the storage and loss moduli had a weak dependency on the frequency. In general, the storage and loss moduli decreased and slowly converged with an increase in the moisture content. The storage and loss moduli decreased with an increasing temperature. The creep-recovery experiment and dynamic shear tests indicated that the pericarps with high moisture contents were more prone to permanent deformation. The dynamic shear tests further demonstrated that a low moisture content, temperature, and frequency resulted in the pericarps having a more solid behavior and undergoing elastic deformation. Images of the microstructure showed that cells in the raw pericarps were round, of similar size, and neatly arranged. In the treated pericarps, the cells gradually became smaller and finally disappeared. It was inferred that drying with hot air caused the loss of intracellular substances, which in turn strengthened the dynamic characteristics of the pericarps. The completely dried pericarps thus behaved as strong viscoelastic solid in contrast to the raw pericarps.

Keywords: Sapindus mukorossi; Viscoelastic behavior; Moisture content; Microstructure; Drying

*Contact information: a: School of Technology, Beijing Forestry University, Beijing 100083, China; b: Key Lab of State Forestry Administration for Forestry Equipment and Automation, Beijing Forestry University, Beijing 100083, China; *Corresponding author: xudaochun@bjfu.edu.cn*

INTRODUCTION

The genus *Sapindus* includes approximately 13 species and is widely distributed in the warmer regions of the Americas, Asia, and Oceania. There are four species and one variety in China that grow in the Yangtze River basin and various provinces in southern China. China has already started developing a large planting area of *Sapindus*, with the area that has been planted reaching nearly 100,000 $h \cdot m^2$. In Fujian Province, the planted area has reached more than 7000 $h \cdot m^2$. More than 1000 $h \cdot m^2$ of *Sapindus* were planted in southern Fujian in 2008, while more than 3000 $h \cdot m^2$ were planted in southern Fujian in 2009 (Jia and Sun 2012).

The literature has reported that *Sapindus mukorossi* pericarp is rich in saponins, with a total saponins yield of up to 33.4% (Wu *et al.* 2015). Saponins are natural surfactants and usually serve as commercial ingredients in cosmetics, washing soaps, and other cleaning products. Saponins are also a class of plant-derived biosurfactant. Biosurfactants are an ideal ecofriendly candidate for cleaning technologies because of their biodegradability and low toxicity (Pacwa-Płociniczak *et al.* 2011). Furthermore, the

extracts of ethyl acetate show strong antibacterial activities against bacteria and dermatophytes (Wu *et al.* 2014).

Lovato *et al.* (2014) reported that *Sapindus* seeds are rich in oil, with the oil yield being approximately 40%. In the extracted oil, the most abundant fatty acid is oleic acid (Sun *et al.* 2017). The oil extracted from *Sapindus* is preferred in the biodiesel industry because of its low production costs. Chakraborty and Baruah (2013) investigated the properties of extracted oil to be used for biodiesel production and showed that *S. mukorossi* has favorable distillation characteristics.

The tyrosinase inhibition, free radical scavenging, anti-microbial, and anti-cancer properties of extracts from *S. mukorossi* seeds have been investigated (Chen *et al.* 2010). These bioactivities demonstrate the high potential of applying these extracts in the fields of medical cosmetology, food supplementation, and antibiotics and chemotherapy. Hu *et al.* (2018) analyzed the antifungal activities of triterpenoid saponins from *S. mukorossi* pulp. An amazing finding was that *S. mukorossi* stem bark can be used for disorders related to inflammation (Shah *et al.* 2017). Moreover, Sunanda *et al.* (2013) used *Sapindus* seed hulls for the preparation of activated carbon.

The viscoelastic properties of fruits and vegetables have been extensively studied in the fields of storage and processing to determine the relationship between processing (storage) and food texture (Lin and Pitt 1986; Jack *et al.* 1995; Jackman and Stanley 1995; Alvarez and Canet 1998; Nieto *et al.* 1998; Martínez *et al.* 2007; Wu and Guo 2010; Xu and Li 2015; Wang *et al.* 2016; Wu *et al.* 2016). Wu *et al.* (2016) investigated the effects of a pretreatment that uses a strong pulsed electric field on the dynamic viscoelasticity of fruits and vegetables. Xu and Li (2015) evaluated the correlations of the viscoelastic behavior with the water state and microstructure of carrots dried with hot air. Wu and Guo (2010) investigated the dynamic viscoelastic behavior and microstructural changes of Korla pears for various turgor levels. Martínez *et al.* (2005), Nieto *et al.* (1998), and Lin and Pitt (1986) investigated the texture of apples and potatoes that were processed in various ways. Alvarez and Canet (1998) studied the rheological properties of fresh and mature potato tissue. Wang *et al.* (2016) studied the rheological properties of different varieties of apple peels and established mathematical models for the relaxation and creep of apple peels. Jackman and Stanley (1995) studied the creep behavior of tomato pericarp tissue affected by ambient-temperature ripening and chilled storage.

Sapindus mukorossi pericarp is rich in saponins, the seed is rich in oil, and the value of *S. mukorossi* as a biomass-energy tree species has been widely studied. However, there are no published studies on the viscoelastic characteristics of *S. mukorossi* pericarp. The dynamic moduli of *S. mukorossi* pericarp indicate energy loss and energy storage when the pericarp is subjected to an external force, and this can directly reflect the resistance of *S. mukorossi* pericarp under different conditions. Furthermore, the results obtained in this work can provide some theoretical guidance for the shelling of the fruit.

In the present study, the viscoelastic behaviors of the pericarp under different conditions were investigated to gain a theoretical basis for the design of a shelling machine. The specific objectives of the research were to investigate the viscoelastic properties of *S. mukorossi* pericarp and analyze the resulting factors. The experimental results will provide valuable information for the design of a machine that is used for shelling and are thus economically important.

EXPERIMENTAL

Materials and Methods

Material preparation

Sapindus mukorossi fruit, as shown in Fig. 1, was harvested in October 2017 in Fujian, China. The fruit was fresh and undamaged, and it was largely mature and uniform in size. Samples were wrapped and then stored in a refrigerator at a temperature of 4 °C to 6 °C. The fruit was removed from storage at the time of the experiments, and the pericarp was separated from the *S. mukorossi* fruit. The pericarps were grouped and numbered. Three groups were placed in an electrical thermostatic drying oven (Shanghai Boxun Industry & Commerce Co. Ltd, Shanghai, China) for 1 h, 2 h, and 3 h at 80 °C, while a fourth group was dried at 80 °C for 6 h, and then removed for weighing (Yuyao Jinnuo Balance Instrument Co. Ltd, Zhejiang, China). The drying process was repeated until a constant weight was reached. Additionally, a control experiment was conducted where a fifth group of pericarps was not dried. Following these steps, the pericarps were peeled and two slices (thickness of 2.0 mm ± 0.5 mm and width of 10 mm ± 1.0 mm) were cut from the center of each pericarp.

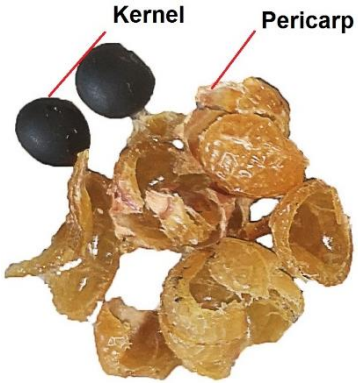

Fig. 1. Fruit of *Sapindus mukorossi*

Moisture content

Complete fruit samples were refrigerated again, but the remaining pericarp was weighed, and the data were recorded as the initial mass (W_1, g). The pericarps were then placed in the drying oven until a constant mass (W_2, g) was obtained. The data reported were the mean values of at least three measurements. The moisture content was considered the same for each pericarp. The moisture content (X_w, %) was calculated with Eq. 1:

$$X_w = (W_1 - W_2) \times 100\% / W_2 \quad (1)$$

Evaluation of the Viscoelastic Properties

The storage modulus (G'), loss modulus (G''), and loss tangent (tan δ) were measured in a shear configuration on a Dynamic Thermomechanical Analyzer DMA Q800 (TA Instruments, Wakefield, MA, USA). Each shear test required two identical slices. To meet the requirements of the shear test, square slices (thickness of 2.0 mm ± 0.5 mm, width of 10 mm ± 1.0 mm, and length of 10 mm ± 1.0 mm) were shaped from the middle of the pericarp using a sharp razor blade. After sample preparation, the size was again checked with Digimatic calipers to avoid large deviations. The frequency sweep test was performed at 0.1 Hz to 100 Hz and lasted 10 min. A room temperature of 22 °C to 23 °C was

maintained. The temperature sweep test was performed at 10 °C to 90 °C and the heating process lasted 20 min. Before starting the test, a preliminary experiment was conducted to obtain the linear viscoelastic region of the pericarp and then select an appropriate amplitude that ensured the material was not damaged. The amplitude was finally set to 3 μm for the test.

In the creep-recovery tests, square samples (thickness of 2.0 mm ± 0.5 mm, width of 10 mm ± 1.0 mm, and length of 10 mm ± 1.0 mm) were compressed using a compression configuration. A constant compressive force of 2 N that lasted 180 s was applied in the tests. A previous force sweep range of 0 N to 2 N was used so that the selected force guaranteed the pericarp was in the linear viscoelastic region. After removal of the force, sample recovery lasted for an additional 180 s. These tests were executed using the DMA Q800.

Theoretical Basis of Viscoelasticity

In the dynamic shear tests, samples were subjected to a sinusoidal change in the stress or strain, while the dynamic mechanical properties of the material were measured. For an ideal elastomer, the strain response to the stress is instantaneous and the strain response is therefore a sinusoidal function that is in phase with the stress. For an ideal viscous body, the strain response of a material lags by $\pi/2\omega$, where ω is the angular velocity. Biomaterials are mostly characterized by the viscoelasticity, and the strain response lags by a certain angle δ, which is within the range 0 to $\pi/2$. The storage modulus, loss modulus, and loss tangent are related according to the following equations,

$$G' = (\sigma / \varepsilon)(\cos \delta) \quad (2)$$

$$G'' = (\sigma / \varepsilon)(\sin \delta) \quad (3)$$

$$\tan \delta = G''/G' \quad (4)$$

where σ is the stress (Pa), ε is the strain of the material, G' is the storage modulus (Pa) that characterizes the energy storage of the material during deformation because of elastic deformation, G'' is the loss modulus (Pa) that characterizes energy loss in the form of heat because of viscous deformation, and tan δ, tan δ is the mechanical loss, which is the ratio of the loss modulus to the storage modulus.

The data were reported as one measurement because one fruit is too small and can only be tested once.

Microstructure

Scanning electron microscopy (SEM) (Zeiss Merlin Fesem, Jena, Germany) was used to examine the *S. mukorossi* samples. After being dried with hot air, the samples had different moisture content and were then placed in a freeze dryer (Thermo Scientific Forma 900 Series, Massachusetts, USA). The freeze dryer was used in order to change the water in the pericarp directly from liquid state to gaseous state, thus to meet the requirements of SEM for the observation environment (that is, the sample does not contain water) and also to ensure that the microstructure was not destroyed by this step. The samples were then cut into small pieces (thickness of 1.5 mm, width of 3 mm, and length of 7 mm) using tweezers and a knife. The samples were fixed on a conductive plate with a conductive adhesive, and then immediately coated with Au (Fig. 2). The samples were firstly placed in the sample room and a vacuuming was performed. Then the operating voltage and working distance was determined. Finally, it was operated on a computer for the microscopy observation.

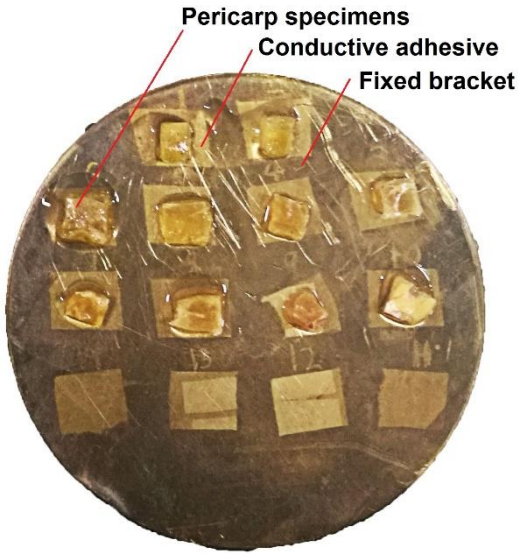

Fig. 2. Specimens for scanning electron microscopy

RESULTS AND DISCUSSIONS

Composition of the Pericarps

Slices of the pericarps were prepared and analyzed with SEM. It was observed that the surface of a pericarp is comprised of agglutinated irregular flakes. The energy spectrum showed that the elemental composition of the *S. mukorossi* pericarp contains carbon (C), oxygen (O), and potassium (K). Figure 3 and Table 1 show that there were large amounts of C and O, while the amount of K was comparatively low. These results were similar to the results published by Borah *et al.* (2017), who conducted an energy-dispersive X-ray analysis to determine the elemental composition of the shell powder from *S. mukorossi*.

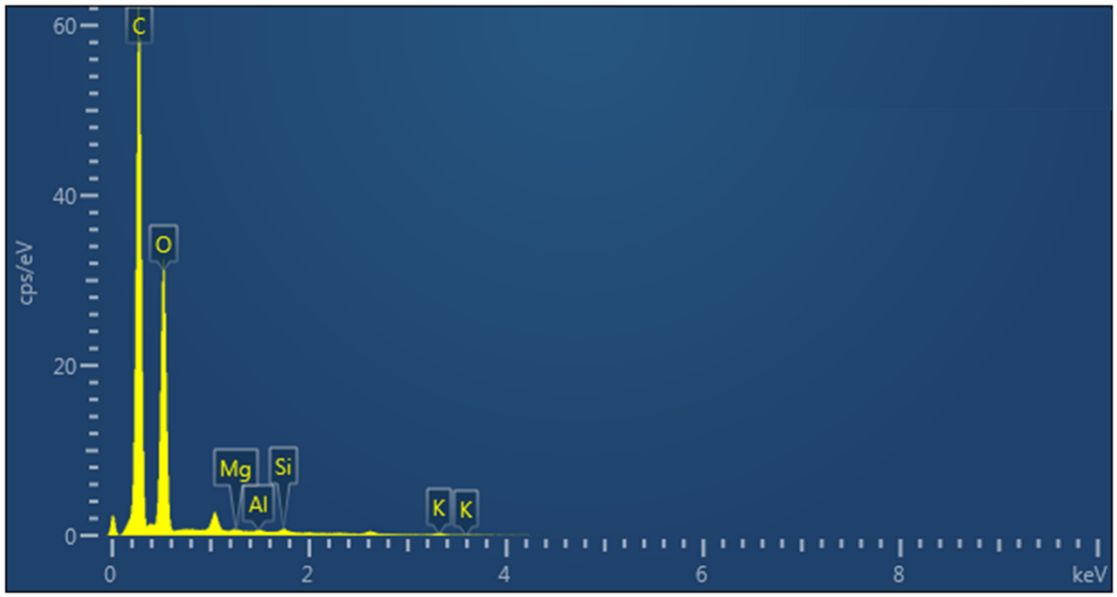

Fig. 3. Energy disperse spectroscopy results

Table 1. Elemental Composition of the *S. mukorossi* Pericarp

Element	wt%	Standard Deviation (wt%)
C	55.46	0.3
O	38.12	0.24
Mg	0.45	0.05
Al	0.32	0.06
Si	0.93	0.08
K	4.71	0.38
Total Amount	100	-

Creep-recovery Response

The creep curves of the *Sapindus* pericarp samples for the different drying times are presented in Fig. 4. Drying with hot air significantly affected ($p < 0.01$, Microsoft Excel Analysis) both the creep strain at 180 s and residual strain after an additional 180 s of recovery. Figure 4 shows that the moisture content of the pericarp had an important effect on the instantaneous viscoelasticity, and there was obvious elastic deformation. With an increasing moisture content, the strain increased, which indicated that the pericarps with a high moisture content were more prone to permanent deformation. The minimum strain value was obtained at a 0% moisture content, which indicated that the totally dried pericarps were the most brittle in this condition and more prone to elastic deformation. These changes were similar to those of the dynamic moduli in the oscillation shear tests. It was further shown that pericarps with a high moisture content were more prone to permanent deformation and conducive to peeling.

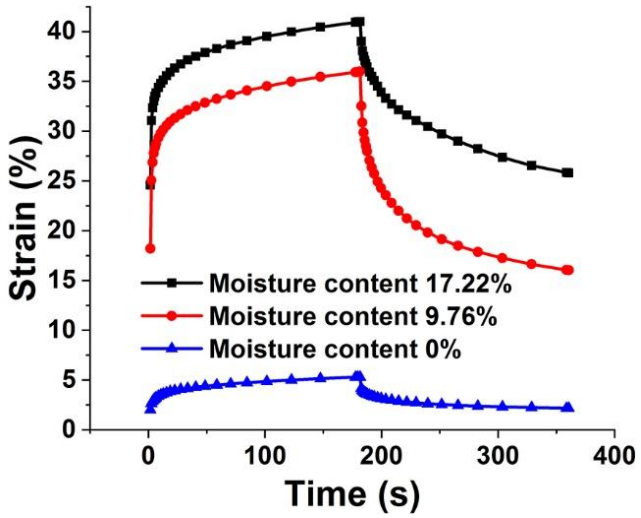

Fig. 4. Creep curves of the *Sapindus* pericarp with different moisture contents

Storage Modulus, Loss Modulus, and Loss Tangent

The pericarps of the samples behaved as a viscoelastic solid with a storage modulus higher than the loss modulus, which indicated a dominant solid behavior of the pericarps. This result was consistent with the viscoelastic behavior of carrot and Korla pear tissues (Martínez *et al*. 2005; Wu and Guo 2010; Xu and Li 2015). However, in some cases, the storage and loss moduli were close, and the differences between the two values were slightly different under different conditions.

Effect of the moisture content on the viscoelasticity

The viscoelasticity curves for different moisture contents obtained from the frequency and temperature scanning are shown in Figs. 5 to 7. Figure 5 shows that the moisture content ranged from 0% to 20%.

The change in the viscoelastic behavior with the moisture content is shown in Fig. 5. The three moduli followed almost the same trend with an increase in the moisture content for both frequency and temperature scanning. The dynamic moduli at different frequencies are shown in Figs. 5a and 5b. The dynamic moduli decreased with an increase in the moisture content, which showed that the tissues became more viscous and elastic after treatment.

These results were different from those for osmotic dehydrated apples and melon tissues (Martínez *et al.* 2005; Loredo *et al.* 2013). When the moisture content was low, the storage modulus greatly exceeded the loss modulus. However, at a higher moisture content, the difference between the two moduli was less. The storage modulus had a sharp and then gentle decline, whereas the loss modulus had a relatively gentle decline across the whole range. The loss tangent had a trend different from the trends of the other two moduli. The loss tangent first increased, reached a maximum at a moisture content of approximately 11%, and then decreased. Furthermore, the frequency tended to have little effect compared with the moisture content.

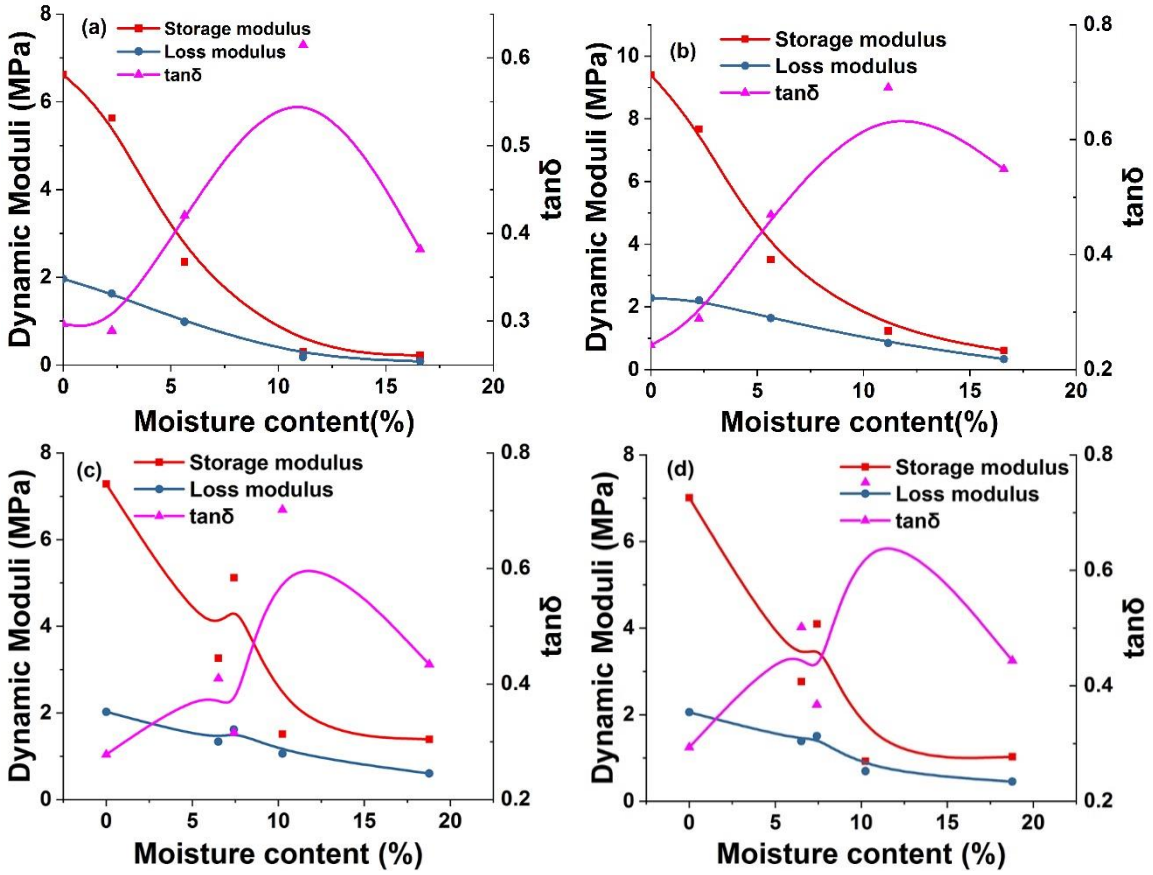

Fig. 5. Dynamic moduli against the moisture content at frequencies of (a) 1 Hz and (b) 50 Hz and temperatures of (c) 10 °C and (d) 30 °C

At different temperatures the trend of the dynamic moduli was probably the same as that at different frequencies. Both the *G*' and *G*" decreased with an increase in the moisture content (Figs. 5c and 5d). The loss tangent first increased and then decreased. However, for the raw pericarps (*i.e.*, pericarps with a higher moisture content), the difference between the storage and loss moduli during temperature scanning was higher than during frequency scanning. This may have been because the temperature scanning was conducted over a period of time that resulted in the loss of water or some material in the pericarps. During temperature scanning, a temperature of 10 ℃ was not the starting point because liquid nitrogen was used to decrease the experimental temperature from room temperature (22 ℃ to 23 ℃) to 10 ℃.

Effect of the frequency on the viscoelasticity

The *G*' had a weak dependency on the frequency (Fig. 6a). This result did not agree with the results for apples reported by Varela *et al.* (2007), who showed the frequency dependency of the *G*' with the storage time for apples. The present results were consistent with the viscoelastic behaviors of apples obtained by Loredo *et al.* (2013) and studies on melon tissue and kiwi fruit (Gerschenson *et al.* 2001; Martínez *et al.* 2005). However, the *G*" had a relatively obvious upward trend with an increasing frequency (Fig. 6b) compared with the *G*'. Pericarps subjected to a high frequency of external forces were more prone to permanent deformation.

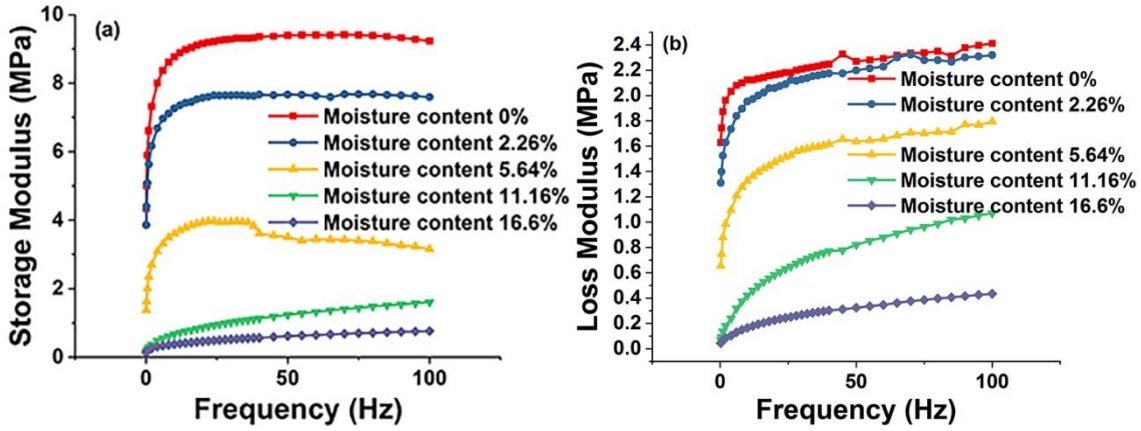

Fig. 6. Frequency *vs*. the (a) storage and (b) loss moduli

Effect of the temperature on the viscoelasticity

The results of the temperature scanning are shown in Fig. 7. The *G*' exceeded the *G*" over the temperature scanning range. Both moduli decreased with an increasing temperature; the *G*' was initially greater than the *G*" (Figs. 7a and 7b). With an increase in the temperature, the two values decreased and slowly converged. When the temperature reached 90 °C, the two values nearly met, which indicated a gel state. The tan δ first increased and then decreased, and the *G*" was finally lower than 0.5 MPa. Figure 7c shows that the storage and loss moduli decreased with an increase in the temperature. The tan δ values in Figs. 7b and 7c first increased and then decreased after reaching a peak at 70 °C to 80 °C. Figure 5d differs from Figs. 7a to 7c in that tan δ first increased, decreased from approximately 30 °C, reached a minimum at approximately 55 °C, and then increased again.

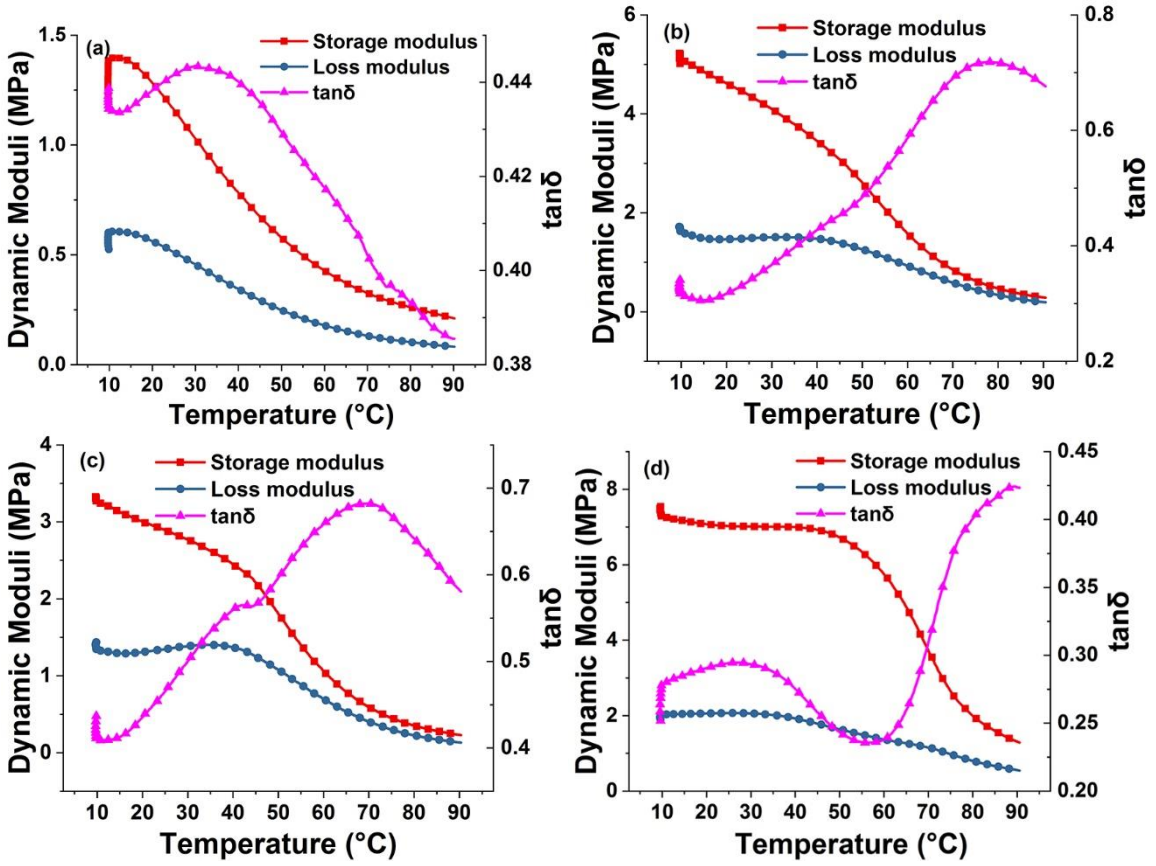

Fig. 7. Dynamic moduli during temperature scanning for different moisture contents: (a) 18.78%, (b) 7.42%, (c) 6.52%, and (d) 0%

In the plotted results, the *G*' and *G*" were initially separated and did not have the same properties as the two above results. This was because during the temperature sweep, the temperature was initially at room temperature, it was then reduced with liquid nitrogen, and the starting point of the curve was therefore not the starting point of the temperature scan. These results showed that with an increase in the temperature, both the *G*' and *G*" decreased, and they were already close to each other at 90 °C, which revealed that an increase in the temperature can shift *S. mukorossi* pericarp into the re-gel state. In this test, heating would cause drying of the material. Because of the difference of the initial moisture content of each specimen, its viscoelastic performance during heating will also vary. It was uncertain whether the pericarps were completely dried during the experiment. In this way, the moisture contents of the pericarps would be equilibrium with the air.

The results showed that the moisture content strongly affected the *G*' and *G*". In contrast to the moisture content, the temperature tended to have little effect on the dynamic moduli. The dynamic moduli had a weak dependence on the frequency. The storage modulus was hardly affected by the frequency. Furthermore, with an increase in the hot-air drying time, the dynamic moduli increased, and thus the pericarps became firmer and tended to undergo more elastic deformation when exposed to an external force. For the raw pericarps, the curves of *G*' and *G*" were close to intersecting, which indicated that the raw pericarp was probably in a gel state. The *G*' tended to remain constant with an increasing frequency, while the *G*" increased slightly with an increasing frequency, which indicated that with an increase in the frequency, the pericarps tended to undergo more permanent

deformation when exposed to an external force. Both of the dynamic moduli decreased with an increasing temperature. This indicated that the pericarps tended to undergo elastic deformation at low temperatures and permanent deformation at high temperatures. In brief, a low temperature, moisture content, and frequency resulted in the pericarps behaving more like a solid and tending to undergo elastic deformation.

SEM

The SEM images showed the changes in the cell microstructure of the raw and dried pericarps (moisture content of 20% to 0%; Figs. 8a to 8d). In the raw pericarps, the cell pores were round, similar in size, and regularly arranged. When a pericarp was dried for 1 h, the moisture content decreased to 8.33%, the cell pores became smaller, and irregularly shaped long holes formed; *i.e.*, the cells became smaller as they were squeezed. When a pericarp was dried for 2 h, the moisture content decreased to 3.36%, the cell pores continued to decrease in size, and the number of cell pores also decreased. There were almost no cells in the completely dried pericarp (Fig. 8d).

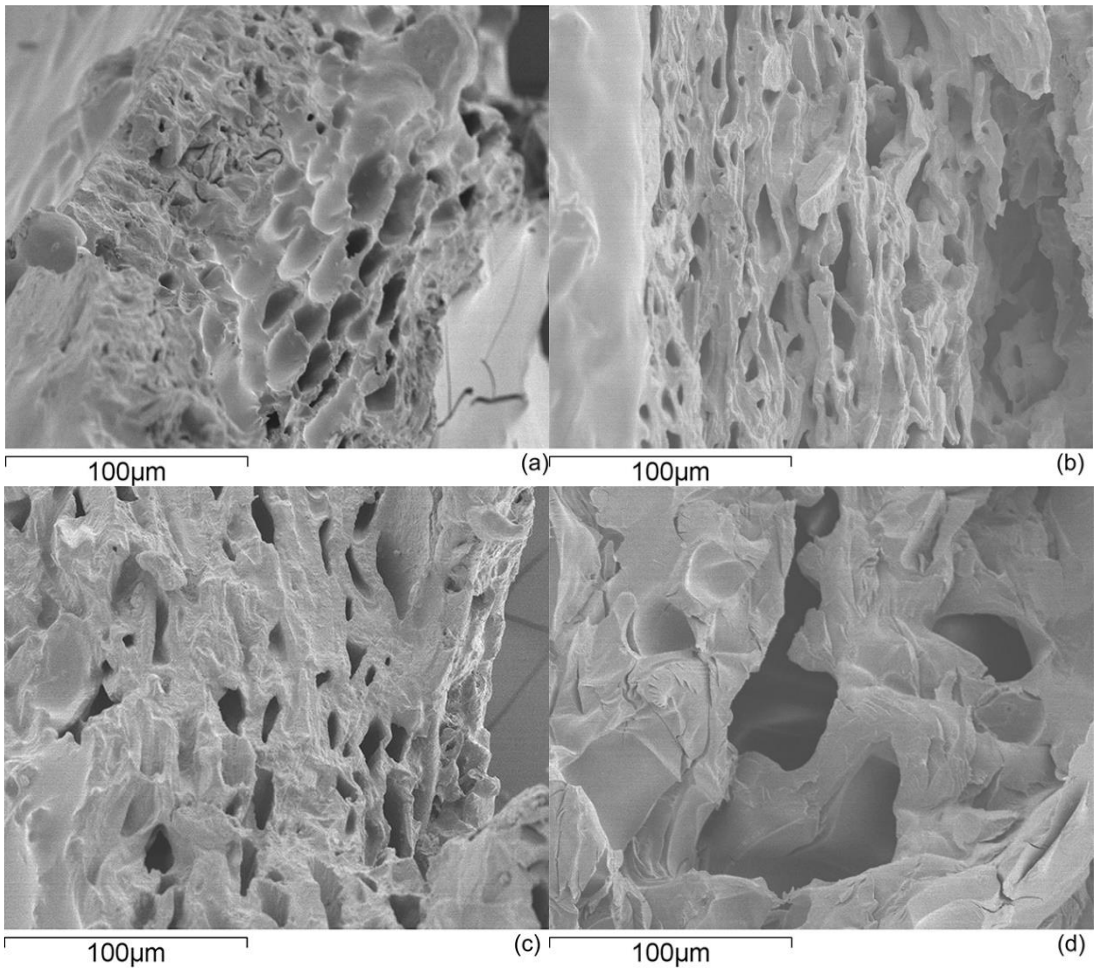

Fig. 8. Microstructure of the pericarps at a moisture content of (a) 19.51%, (b) 8.33%, (c) 3.36%, and (d) 0%

The SEM images show that the cells of the pericarps may have contained substances that keep the cells in a rounded plump state. The smaller cells may have resulted from the loss of intracellular material because of drying in hot air; the intracellular pressure

decreased, and thus the cells became smaller. There were large holes in the completely dried pericarp (Fig. 8d), and it was speculated that these holes were squeezed and became cracks because of the complete loss of intracellular material, and some pores disappeared.

Drying treatment may cause the loss of cellulose molecules that are the main component of the cell wall, and these losses result in a loss of firmness (Phothiset and Charoenrein 2014). However, in the present study, the drying process increased the dynamic moduli. It was speculated that a loss of cellulose molecules resulted in a loss of firmness. However, the intracellular substances accounted for the main elastic and viscous characteristics, and the loss of these substances arranged the tissue of the pericarps more closely and increased the density. The dynamic moduli of the pericarps thus increased, and the cell elasticity became more dominant.

CONCLUSIONS

1. This study revealed that the pericarps behaved as a viscoelastic solid with a storage modulus higher than the loss modulus. (The typical range of tan δ value is from 0.2 to 0.7.) A low temperature, moisture content, and frequency resulted in the pericarps behaving more like a solid and undergoing elastic deformation. In contrast, a high temperature, moisture content, and frequency resulted in the pericarps being less stiff and thus undergoing permanent deformation when exposed to an external force.
2. The moisture content strongly affected the viscoelastic behavior of *S. mukorossi* pericarps. Both the creep-recovery tests and dynamic shear tests demonstrated that the pericarps with high moisture contents were more prone to permanent deformation.
3. Compared to moisture content, the temperature during testing tended to have little effect on the dynamic moduli. The dynamic moduli weakly depended on the frequency (0.1 Hz to 100 Hz). The pericarps were more likely to undergo permanent deformation at a higher frequency.
4. The images of the microstructure showed that the cells in the raw pericarps were round, of similar size, and neatly arranged. The cells of the treated pericarps gradually became smaller with an increasing hot-air drying time and finally connected with each other to form cracks or were squeezed sufficiently to disappear. It was inferred that drying in hot air resulted in the loss of intracellular substances, which can strengthen the dynamic characteristics of the pericarps. The completely dried pericarps behaved as a strong viscoelastic solid in contrast to the raw pericarps.
5. The above data on the viscoelasticity of the pericarps can provide a theoretical basis for the design of a shelling machine with different moisture contents. The pericarps were more prone to elastic deformation when the moisture content was low; therefore, it was concluded dried pericarps are more easily broken by extrusion, while fresh fruit are more prone to being cut by a cutter. This is practically useful for the design of a sheller. Thus, the next work is to apply these findings for the design of a shelling machine.

ACKNOWLEDGEMENTS

This work was supported by the Fundamental Research Funds for the Central Universities (No. 2015ZCQ-GX-02). The authors thank Glenn Pennycook, MSc, from Liwen Bianji, Edanz Group, China (www.liwenbianji.cn/ac), for editing the English text of a draft of this manuscript.

REFERENCES CITED

Alvarez, M. D., and Canet, W. (1998). "Rheological characterization of fresh and cooked potato tissues (cv. Monalisa)," *Z. Lebensm. Unters. F. A.* 207(1), 55-65. DOI: 10.1007/s002170050295

Borah, R. K., Mahanta, A., Dutta, A., Bora, U., and Thakur, A. J. (2017). "A green synthesis of palladium nanoparticles by *Sapindus mukorossi* seed extract and use in efficient room temperature Suzuki-Miyaura cross-coupling reaction," *Appl. Organomet. Chem.* 31(11). DOI: 10.1002/aoc.3784

Chakraborty, M., and Baruah, D. C. (2013). "Production and characterization of biodiesel obtained from *Sapindus mukorossi* kernel oil," *Energy* 60, 159-167. DOI: 10.1016/j.energy.2013.07.065

Chen, C.-Y., Kuo, P.-L., Chen, Y.-H., Huang J.-C., Ho, M.-L., Lin, R.-J., Chang, J.-S., and Wang, H.-M. (2010). "Tyrosinase inhibition, free radical scavenging, antimicroorganism and anticancer proliferation activities of *Sapindus mukorossi* extracts," *J. Taiwan Inst. Chem. E.* 41(2), 129-135. DOI: 10.1016/j.jtice.2009.08.005

Gerschenson, L. N., Rojas, A. M., and Marangoni, A. G. (2001). "Effects of processing on kiwi fruit dynamic rheological behaviour and tissue structure," *Food Res. Int.* 34(1), 1-6. DOI: 10.1016/S0963-9969(00)00121-6

Hu, Q., Chen, Y.-Y., Jiao, Q.-Y., Khan, A., Li, F., Han, D.-F., Cao, G.-D., and Lou, H.-X. (2018). "Triterpenoid saponins from the pulp of *Sapindus mukorossi* and their antifungal activities," *Phytochemistry* 147, 1-8. DOI: 10.1016/j.phytochem.2017.12.004

Jack, F. R., Paterson, A., and Piggott, J. R. (1995). "Perceived texture: Direct and indirect methods for use in product development," *Int. J. Food Sci. Tech.* 30(1), 1-12. DOI: 10.1111/j.1365-2621.1995.tb01939.x

Jackman, R. L., and Stanley, D. W. (1995). "Creep behavior of tomato pericarp tissue as influenced by ambient temperature ripening and chilled storage," *J. Texture Stud.* 26(5), 537-552. DOI: 10.1111/j.1745-4603.1995.tb00802.x

Jia, L., and Sun, C. (2012). "Research progress of biodiesel tree *Sapindus mukorossi*," *J. China Agric. Univ.* 17(6), 191-196.

Lin, T.-T., and Pitt, R. E. (1986). "Rheology of apple and potato tissue as affected by cell turgor pressure," *J. Texture Stud.* 17(3), 291-313. DOI: 10.1111/j.1745-4603.1986.tb00554.x

Loredo, A. B. G., Guerrero, S. N., Gomez, P. L., and Alzamora, S. M. (2013). "Relationships between rheological properties, texture and structure of apple (Granny Smith var.) affected by blanching and/or osmotic dehydration," *Food Bioprocess Tech.* 6(2), 475-488. DOI: 10.1007/s11947-011-0701-9

Lovato, L., Pelegrini, B. L., Rodrigues, J., de Oliveira, A. J. B., and Ferreira, I. C. P. (2014). "Seed oil of *Sapindus saponaria* L. (Sapindaceae) as potential C16 to C22 fatty acids resource," *Biomass Bioenerg.* 60, 247-251. DOI: 10.1016/j.biombioe.2013.11.016

Martínez, V. Y., Nieto, A. B., Castro, M. A., Salvatori, D., and Alzamora, S. M. (2007). "Viscoelastic characteristics of Granny Smith apple during glucose osmotic dehydration," *J. Food Eng.* 83(3), 394-403. DOI: 10.1016/j.jfoodeng.2007.03.025

Martínez, V. Y., Nieto, A. B., Viollaz, P. E., and Alzamora, S. M. (2005). "Viscoelastic behavior of melon tissue as influenced by blanching and osmotic dehydration," *J. Food Sci.* 70(1), E12-E18. DOI: 10.1111/j.1365-2621.2005.tb09031.x

Nieto, A., Salvatori, D., Castro, M. A., and Alzamora, S. M. (1998). "Air drying behavior of apples as affected by blanching and glucose impregnation," *J. Food Eng.* 36(1), 63-79. DOI: 10.1016/S0260-8774(98)00043-0

Pacwa-Płociniczak, M., Płaza, G. A., Piotrowska-Seget, Z., and Cameotra, S. S. (2011). "Environmental applications of biosurfactants: Recent advance," *Int. J. Mol. Sci.* 12(1), 633-654. DOI: 10.3390/ijms12010633

Phothiset, S., and Charoenrein, S. (2014). "Effects of freezing and thawing on texture, microstructure and cell wall composition changes in papaya tissues," *J. Sci. Food Agr.* 94(2), 189-196. DOI: 10.1002/jsfa.6226

Shah, M., Parveen, Z., and Khan, M. R. (2017). "Evaluation of antioxidant, anti-inflammatory, analgesic and antipyretic activities of the stem bark of *Sapindus mukorossi*," *BMC Complem. Altern. M.* 17(1), 526-541. DOI: 10.1186/s12906-017-2042-3

Sun, C., Jia, L., Xi, B., Wang, L., and Weng, X. (2017). "Natural variation in fatty acid composition of *Sapindus* spp. seed oils," *Ind. Crop. Prod.* 102, 97-104. DOI: 10.1016/j.indcrop.2017.03.011

Sunanda, Tiwari, D. P., Sharma, D. N., and Kumar, R. T. S. (2013). "*Sapindus* based activated carbon by chemical activation," *Res. J. Mater. Sci.* 1(7), 9-15.

Varela, P., Salvador, A., and Fiszman, S. (2007). "Changes in apple tissue with storage time: Rheological, textural and microstructural analyses," *J. Food Eng.* 78(2), 622-629. DOI: 10.1016/j.jfoodeng.2005.10.034

Wang, J., Cui, Q., Li, H., Liu, Y., and Wang, Y. (2016). "Evaluation on peels texture of different apple cultivars based on rheological properties," *Transactions of the Chinese Society of Agricultural Engineering* 32(21), 305-314.

Wu, H., Zhang, L., Wang, N., Guo, Y., Weng, Z., Sun, Z., Xu, D., Xie, Y., and Yao, W. (2014). "Analysis of the bioactive components of *Sapindus saponins*," *Ind. Crop. Prod.* 61, 422-429. DOI: 10.1016/j.indcrop.2014.07.026

Wu, H., Zhang, L., Wang, N., Guo, Y., Weng, Z., Sun, Z., Xu, D., Xie, Y., and Yao, W. (2015). "Extraction and fermentation-based purification of Saponins from *Sapindus mukorossi* Gaertn.," *J. Surfactants Deterg.* 18(3), 429-438. DOI: 10.1007/s11743-015-1668-8

Wu, J., and Guo, K. Q. (2010). "Dynamic viscoelastic behaviour and microstructural changes of Korla pear (*Pyrus bretschneideri rehd*) under varying turgor levels," *Biosyst. Eng.* 106(4), 485-492. DOI: 10.1016/j.biosystemseng.2010.05.014

Wu, X., Guo, Y., and Feng, H. (2016). "Effect of high pulsed electric field pretreatment on dynamic viscoelasticity of fruits and vegetables," *Transactions of the Chinese Society of Agricultural Engineering* 32(18), 247-254. DOI: 10.11975/j.issn.1002-6819.2016.18.034

Xu, C., and Li, Y. (2015). "Correlation of viscoelastic behavior with water state and ultrastructure in hot air-dried carrots," *Food Control* 50, 23-30.
DOI: 10.1016/j.foodcont.2014.08.020

Article submitted: December 15, 2018; Peer review completed: March 16, 2019; Revised version received and accepted: March 24, 2019; Published: March 28, 2019.
DOI: 10.15376/biores.14.2.3961-3974